Journal of Hazardous Materials 243 (2012) 19–27

Contents lists available at SciVerse ScienceDirect

Journal of Hazardous Materials

journal homepage: www.elsevier.com/locate/jhazmat

Ovarian dysfunction and gene-expressed characteristics of female mice caused by long-term exposure to titanium dioxide nanoparticles

Guodong Gao[a,b,1], Yuguan Ze[a,1], Bing Li[a,1], Xiaoyang Zhao[a,1], Ting Zhang[c,d,1], Lei Sheng[a], Ringhu Hu[a], Suxin Gui[a], Xuezi Sang[a], Qingqing Sun[a], Jie Cheng[a], Zhe Cheng[a], Ling Wang[a], Meng Tang[c,d,*], Fashui Hong[a,**]

[a] Medical College, Soochow University, Suzhou 215123, People's Republic of China
[b] Shangrao Branch of Jiangxi Medical College, People's Republic of China
[c] Key Laboratory of Environmental Medicine and Engineering, Ministry of Education, School of Public Health, Southeast University, Nanjing 210009, People's Republic of China
[d] Jiangsu key Laboratory for Biomaterials and Devices, Southeast University, Nanjing 210009, People's Republic of China

HIGHLIGHTS

- Exposure to TiO_2 NPs could be significantly accumulated in ovary.
- Exposure to TiO_2 NPs caused ovarian injury in mice.
- Exposure to TiO_2 NP decreased fertility or the pregnancy rate.
- Exposure to TiO_2 NP resulted in imbalance of sex hormones in mice.
- Exposure to TiO_2 NP caused alteration of 228 genes expression of known function in ovary.

ARTICLE INFO

Article history:
Received 11 February 2012
Received in revised form 8 July 2012
Accepted 21 August 2012
Available online 11 September 2012

Keywords:
Titanium dioxide nanoparticles
Ovary
Fertility
Sex hormones
Gene-expressed profile

ABSTRACT

Although numerous studies have described the accumulation of titanium dioxide nanoparticles (TiO_2 NPs) in the liver, kidneys, lung, spleen, and brain, and the corresponding damage, it is unclear whether or not TiO_2 NPs can be translocated to the ovary and cause ovarian injury, thus impairing fertility. In the current study, ovarian injury and gene-expressed characteristics in female mice induced by intragastric administration of TiO_2 NPs (10 mg/kg) for 90 consecutive days were investigated. Our findings indicated that TiO_2 NPs can accumulate in the ovary and result in ovarian damage, cause an imbalance of mineral element distribution and sex hormones, decrease fertility or the pregnancy rate and oxidative stress in mice. Microarray analysis showed that in ovaries from mice treated with TiO_2 NPs compared to controls, 223 genes of known function were up-regulated, while 65 ovarian genes were down-regulated. The increased expression of *Cyp17a1* following TiO_2 NPs treatment suggested that the increase in estradiol biosynthesis may be a consequence of increased TiO_2 NPs. In addition, the elevated expression of *Akr1c18* implied that progesterone metabolism was accelerated, thus causing a decrease in the progesterone concentration. Taken together, the apparent regulation of key ovarian genes supports the hypothesis that TiO_2 NPs directly affects ovarian function.

1. Introduction

Nanotechnology provides driving force to progress in life sciences and information technology. However, several studies have called attention to the potential hazards arising from nanotechnology [1–4]. For the past few years, titanium dioxide nanoparticles (TiO_2 NPs) have increasingly been used in cosmetics, food additives, drug delivery vehicles, bio-medical ceramics and implanted biomaterial paints, waste water treatment, and sterilization, largely due to their appropriate physicochemical properties. The toxicity of TiO_2 NPs is associated with their physicochemical properties (e.g., size, surface area, and crystal phase) [5]. Some studies have reported that TiO_2 NPs enter the systemic circulation, migrate to various organs and tissues, and exert adverse effects [6–9]. Our previous studies have also shown that TiO_2 NPs exposure results in accumulation and damage in the liver, spleen, and kidneys of female mice [10–19].

* Corresponding author at: Jiangsu key Laboratory for Biomaterials and Devices, Southeast University, Nanjing 210009, People's Republic of China.
** Corresponding author. Tel.: +86 0512 61117563; fax: +86 0512 65880103.
E-mail address: Hongfsh_cn@sina.com (F. Hong).
[1] Guodong Gao, Yuguan Ze, Bing Li, Xiaoyang Zhao, and Ting Zhang contributed equally to this work.

0304-3894/$ – see front matter.
http://dx.doi.org/10.1016/j.jhazmat.2012.08.049

We also demonstrated that TiO_2 NPs were translocated to the brain and caused injury in female mice [20–22], which may have effects on hormone secretion in the pituitary gland and female reproduction; however, whether or not TiO_2 NPs can be translocated to the ovaries of mammals and affect reproduction is unknown. Recently, the toxicologic characteristics of some nanomaterials in ovarian cells *in vitro* have been reported. For instance, gold nanoparticles were shown to enter rat ovarian granulosa cells and subcellular organelles and alter estrogen accumulation *in vitro* [23], and were able to traverse the cell membrane and enter Chinese hamster ovary cells by the endocytic pathway [24]. In addition, calcium phosphate nanoparticles entered granulosa cells, and were distributed in the membranous compartments, including lysosome, mitochondria and intracellular vesicles, affected hormone production, and caused apoptosis in human granulosa cells [25]. Silicon carbide nanowires induced activation of mitogen-activated protein kinase cellular signal transduction pathways in mammalian cells [26], and confocal laser scanning microscopy observations showed that the TiO_2 NPs easily moved to the cytoplasm of cultured Chinese hamster ovary cells, and not to the nucleus [27]. TiO_2 or Al_2O_3 NPs agglomerated on both the surface and inside of Chinese hamster ovary cells and induced genotoxicity and cytotoxicity in these cells [28]. The widespread occurrence of TiO_2 NPs, albeit in minimal amounts, in the environment and in cosmetics makes the general population vulnerable to exposure. Exposure to TiO_2 NPs can occur via inhalation, transdermal absorption, and ingestion, therefore, we speculate that the ovary might also be one of the target organs of toxicity in mammals exposed to TiO_2 NPs.

The aim of the present study was to evaluate ovarian dysfunction and its gene-expressed profile following TiO_2 NPs exposure as a possible mechanism of ovarian injury. The toxicogenomic approach was used to determine the effects of TiO_2 NPs exposure on ovarian gene expression by microarray analysis. The examination of ovarian gene expression provides a full understanding of the effects of TiO_2 NPs on the mouse ovary.

2. Materials and methods

2.1. Preparation and characterization of TiO_2 NPs

Nanoparticulated anatase TiO_2 was prepared via controlled hydrolysis of titanium tetrabutoxide. The details of the synthesis and characterization of TiO_2 NP have been previously described by our group [20,29]. TiO_2 powder was dispersed on the surface of 0.5% (w/v) hydroxypropylmethylcellulose (HPMC) K4M solution, and the solutions containing TiO_2 particles were treated ultrasonically for 15–20 min and then mechanically vibrated for 2 or 3 min. X-ray-diffraction (XRD) patterns of TiO_2 NPs were obtained at room temperature with a MERCURY CCD diffractometer (MERCURY CCD Co., Japan) using Ni-filtered Cu Kα radiation. The particle sizes of both the powder and the nanoparticles suspended in 0.5% (w/v) HPMC solution after incubation for 12 h and 24 h (5 mg/ml) were determined using a TecnaiG220 transmission electron microscope (TEM) (FEI Co., USA) operating at 100 kV, respectively. Mean particle size was determined by measuring more than 100 individual particles which were randomly sampled. XRD measurements showed that TiO_2 NPs exhibit the anatase structure, and the average grain size calculated from the broadening of the (1 0 1) XRD peak of anatase was approximately 6 nm using Scherrer's equation. TEM demonstrated that the average particle size of the powder suspended in HPMC solvent after 12 h and 24 h incubation ranged from 5 to 6 nm. The surface area of the sample was 174.8 m^2/g. The mean hydrodynamic diameter of TiO_2 NP in HPMC solvent ranged from 208 to 330 nm (mainly 294 nm), and the zeta potential after 12 and 24 h incubation was 7.57 and 9.28 mV, respectively [20].

2.2. Animals and treatment

CD-1 (ICR) female mice were used in this study. One hundred fifty CD-1 (ICR) female mice (23 ± 2 g) were purchased from the Animal Center of Soochow University (China). All mice were housed in stainless steel cages in a ventilated animal room. The room temperature of the housing facility was maintained at 24 ± 2 °C with a relative humidity of 60 ± 10% and a 12-h light/dark cycle. Distilled water and sterilized food were available *ad libitum*. Prior to dosing, the mice were acclimated to the environment for 5 days. All procedures used in animal experiments conformed to the U.S. National Institutes of Health Guide for the Care and Use of Laboratory Animals [30] Studies were approved by the Soochow University Institutional Animal Care and Use Committee.

In our preliminary experiments, TiO_2 NP suspensions at different concentrations (2.5, 5, and 10 mg/kg of body weight [BW]) were administered to mice by intragastric administration for 90 consecutive days. Treatment with 10 mg/kg BW TiO_2 NPs resulted in the most severe organ damage [22,31], which was used as the highest concentration for further experiments. The mice were randomly divided into 2 groups ($N = 30$), including the control group (treated with 0.5% (w/v) HPMC) and experimental group (10 mg/kg BW TiO_2 NPs). The mice were weighed, and the TiO_2 NP suspensions were administered to the mice by intragastric administration every day for 90 days. All symptoms and deaths were observed and carefully recorded every day during the 90 days. In addition, after 90 days, the fertility of treated females (10) was tested by caging with males (10) of proven fertility.

After the 90-day period, all mice were weighed and then sacrificed after being anesthetized with ether. Blood samples were collected from the eye vein by rapidly removing the eyeball. Serum was collected by centrifuging blood at 2500 rpm for 10 min. The ovaries were quickly removed and placed on ice and then dissected and frozen at −80 °C.

2.3. Elemental content analysis

The ovaries were removed from the freezer (80 °C) and thawed. Approximately 0.1 g of the ovary was weighed, digested, and analyzed for elemental content. Inductively coupled plasma-mass spectrometry ([ICP-MS] Thermo Elemental X7; Thermo Electron Co., USA) was used to analyze the titanium, sodium, magnesium, potassium, calcium, zinc, and iron concentrations in the samples.

2.4. Histopathologic evaluation of the ovaries

For pathologic studies, all histopathologic examinations were performed using standard laboratory procedures. The ovaries were embedded in paraffin blocks, then sliced (5 μm thickness) and placed onto glass slides. After hematoxylin–eosin (HE) staining, the stained sections were evaluated by a histopathologist unaware of the treatments, using an optical microscope (Nikon U-III Multipoint Sensor System, Japan).

2.5. Observation of ovarian ultrastructure by TEM

Ovaries were fixed in a fresh solution of 0.1 M sodium cacodylate buffer containing 2.5% glutaraldehyde and 2% formaldehyde followed by a 2 h fixation period at 4 °C with 1% osmium tetroxide in 50 mM sodium cacodylate (pH 7.2–7.4). Staining was performed overnight with 0.5% aqueous uranyl acetate. The specimens were dehydrated in a graded series of ethanol (75%, 85%, 95%, and 100%), and embedded in Epon 812. Ultrathin sections were obtained, contrasted with uranyl acetate and lead citrate, and observed with a Hitachi H600 TEM (Hitachi Co., Japan). Ovarian apoptosis was

determined based on the changes in nuclear morphology (e.g., chromatin condensation and fragmentation).

2.6. ROS and DNA oxidation assay of ovary

The assays of ROS (O_2^- and H_2O_2) production in ovaries were spectrophotometrically measured with a commercially available kit (Nanjing Jiancheng Bioengineering Institute, Jiangsu, China).

Ovary DNA was extracted using DNeasy Tissue Mini Kit (Nanjing Jiancheng Bioengineering Institute, Jiangsu, China) as described by the manufacturer. The concentration of DNA was determined by measuring absorbance at 260 nm using a DNA spectrophotometer (Hitachi Co., Japan). Approximately 38 μl of DNA suspension was incubated at 100 °C for 2 min, treated with 3 μl of 250 mM potassium acetate buffer (pH 5.4), 3 μl of 10 mM zinc sulfate, and 2 μl of nuclease P1 (6.25 U/μl; Sigma–Aldrich) at 37 °C overnight, and then treated with 6 μl of 0.5 M Tris–HCl (pH 8.3) and 2 μl of alkaline phosphatase (0.31 U/μl; Sigma–Aldrich), at 37 °C for 2 h. The formation of 8-OHdG was determined using the 8-OHdG ELISA kit (Japan Institute for the Control of Aging, Haruoka, Japan). This kit provides a competitive immunoassay for quantitative measurement of the oxidative DNA adduct 8-OHdG. It was carefully performed according to manufacturer's instructions using a microplate varishaker-incubator, an automated microplate multireagent washer, and a computerized microplate reader.

2.7. Sex hormone assays

Sex hormones were evaluated with serum levels of estradiol (E_2), progesterone (P_4), luteinizing hormone (LH), follicle stimulating hormone (FSH), prolactin (PRL), testosterone (T), and sex hormone binding globulin (SHBG) using commercial kits (Bühlmann Laboratories, Switzerland). All biochemical assays were performed using a clinical automatic chemistry analyzer (Type 7170A; Hitachi Co., Japan).

2.8. Microarray assay

Gene expression profiles for ovarian tissue isolated from control and TiO_2 NPs-treated mice were compared by microarray analysis using an Illumina BeadChip (Affymetrix, Santa Clara, CA, USA). Total RNA was isolated using an Ambion Illumina RNA Amplification Kit (cat#1755; Affymetrix) according to the manufacturer's protocol, and stored at −80 °C. RNA amplification has become the standard method for preparing RNA samples for array analysis [32]. Total RNA was then submitted to Biostar Genechip Inc. (Shanghai, China), where RNA quality was analyzed using a BioAnalyzer and cRNA was generated and labeled using the one-cycle target labeling method. cRNA from each mouse was hybridized to a single array according to the standard Illumina RNA Amplification Kit protocol for a total array.

An Illumina BeadStudio Application was used to analyze data generated in this study. This program identifies differentially expressed genes and establishes the biological significance based on the Gene Ontology (GO) Consortium (http://www.geneontology.org/GO.doc.html). Differentially expressed genes were identified using Student's *t*-test (two-tailed, unpaired), and a threshold of 13.0 was used to limit the data set to genes up- or down-regulated with a diffscore ≥13 or ≤−13.

2.9. Quantitative real-time PCR (qRT-PCR)

The levels of mRNA expression of *Apoe*, *Bmf*, *Calm3*, *Cyp11a*, *Cyp11a1*, *Cyp17a1*, *Cyp2f2*, *Cyp4f18*, *Degs2*, *Foxn4*, *Lgmn*, *Scarb1*, and *Star 2* in the mouse ovary were determined using a real-time quantitative RT polymerase chain reaction (RT-PCR) [33–35]. Synthesized cDNA was used for real-time PCR by employing primers that were designed using Primer Express Software, according to the software guidelines; PCR primer sequences are available upon request.

3. Statistical analysis

Statistical analyses were performed using SPSS 19 software. Data are expressed as the means ± standard error (SE). One-way analysis of variance (ANOVA) was carried out to compare the differences of means among the multi-group data. Dunnett's test was performed when each dataset was compared with the solvent-control data. Statistical significance for all tests was judged at a probability level of 0.05 ($P < 0.05$).

4. Results

4.1. Titanium and mineral element content

The content of titanium in mouse ovaries is shown in Table 1. Titanium accumulated in the ovaries, while no titanium was detected in non-exposed mice.

The content of ovarian mineral elements, including Ca, Na, K, Mg, Zn, Cu, and Fe, was determined and is listed in Table 1. These elements are important building blocks for cells and play important roles in ovarian physiology. The changes in these elements can provide useful information on the physiology and pathology of ovaries. As shown in Table 1, TiO_2 NPs exposure resulted in increased content of Ca, Na, K, and Zn, and decreased content of Mg, Cu, and Fe in the ovary ($P < 0.05$).

4.2. Fertility and development of young mice

Table 2 shows the changes in fertility and development of young mice caused by exposure to TiO_2 NPs. TiO_2 NPs exposure resulted in significant decreases in the mating rate, pregnancy rate, number giving birth, and number of fetuses ($P < 0.05$). Twenty-eight days after birth, the survival rate and body weight of young mice were significantly decreased compared with control mice ($P < 0.05$). These results suggest that TiO_2 NPs exposure decreased fertility and development of young mice.

4.3. Reproductive endocrinology

The levels of sex hormones in the sera of female mice were detected and are listed in Table 3. TiO_2 NPs exposure caused significant increases in E_2 and FSH, and reduction of P_4, LH, and T ($P < 0.05$); however, the levels of PRL and SHBG had no significant changes ($P > 0.05$). The results suggest that TiO_2 NPs impaired the equilibrium of sex hormones in female mice.

4.4. Histopathologic evaluation

The ovarian histopathologic changes are shown in Fig. 1. Significant histopathologic changes were observed in the ovarian tissue compared with the control; specifically, the ovarian tissue had abnormal pathologic changes, including ovarian atrophy, disturbance of primary and second follicle development, irregular arrangement of cells, and a shapeless follicular antrum, suggesting that the ovaries were damaged by long-term exposure to TiO_2 NPs.

Table 1
Accumulation of metal elements in the mouse ovary after an intragastric administration with 10 mg/kg BW TiO_2 NPs for 90 consecutive days.

Treatment	Metal element contents (ng/g tissue)							
	Ti	Ca	Na	K	Mg	Zn	Cu	Fe
Control	Not detectable	245.52 ± 12.28	6214 ± 311	1411 ± 70	269.4 ± 13.47	87.44 ± 4.37	72.31 ± 3.08	312.4 ± 15.62
TiO_2 NPs	3.26 ± 0.16	280.00 ± 14.00*	9112 ± 456*	2387 ± 119**	248.36 ± 12.41	107.59 ± 5.38*	61.58 ± 3.08*	257.22 ± 12.86*

Values represent means ± SE (N = 5).
* Significantly different from the control (unexposed mice) at the 5% confidence level.
** Significantly different from the control (unexposed mice) at the 1% confidence level.

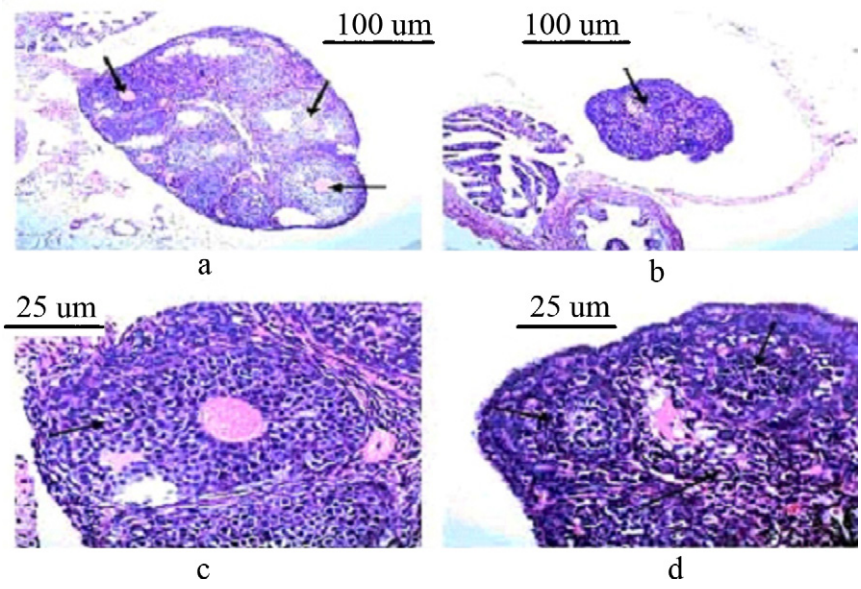

Fig. 1. Histopathological observation of ovary caused by an intragastric administration with 10 mg/kg BW TiO_2 NPs for 90 consecutive days. (a) Control group (unexposed mice): presents normal, regularity of ovarian follicle arrangement, normal of follicle development (black arrow shows); (b) TiO_2 NPs group: ovarian atrophy, no distinct ovarian follicle, and premature ovarian failure (black arrow shows); (c) control group: ovarian follicle presents normal (black arrow shows); and (d) TiO_2 NPs group: atresia of primary and second follicle development, irregularity of ovarian follicle arrangement (black arrow shows), blur of ovarian structure.

4.5. Observation of ovarian ultrastructure

The changes in ovarian cell ultrastructure in mouse ovaries are presented in Fig. 2. It was observed that untreated mouse ovaries (in the control group) contained elliptical nuclei with homogeneous chromatin (Fig. 2a); however, ultrastructure of ovarian cells exposed to TiO_2 NPs indicated mitochondrial swelling and cristae breakage, nucleus chromatin condensation and margination, and irregularity of the nuclear membrane (Fig. 2b). The results suggest that TiO_2 NPs exposure resulted in ovarian apoptosis. In addition, TiO_2 NPs conglomerates in the cytoplasm and nuclei of ovarian cells were observed (Fig. 2b), indicating that TiO_2 NPs were deposited in ovarian cells.

4.6. ROS accumulation and DNA peroxide levels

The effect of treatment with various doses of TiO_2 NPs on the rate of O_2^- and H_2O_2 generation, and DNA damage (8-OHdg) in mouse ovary are shown in Table 4. Significant ROS production and an increase in 8-OHdg in the ovary caused by TiO_2 NPs were observed (P < 0.05 or 0.01), demonstrating that ROS accumulation led to DNA peroxidation and apoptosis in the ovary under TiO_2 NPs-induced toxicity.

Table 2
Effects of TiO_2 NPs on conception of female mice and development of young mice after an intragastric administration with 10 mg/kg BW TiO_2 NPs for 90 consecutive days.

Index	Control	TiO_2 NPs
Mating rate (%)	100 ± 5	70 ± 3.5*
Pregnancy rate (%)	100 ± 5	60 ± 3*
Number of giving birth/fetus	13 ± 0.65	7 ± 0.35**
Survival rate of young mice after 28 days (%)	98.51 ± 4.93	70.83 ± 3.54**
Body weight of young female mice after birth 28 days (g)	14.85 ± 0.74	10.73 ± 0.54*
Body weight of young male mice after birth 28 days (g)	15.91 ± 0.80	10.98 ± 0.55*

Values represent means ± SE (N = 10).
* Significantly different from the control (unexposed mice) at the 5% confidence level.
** Significantly different from the control (unexposed mice) at the 1% confidence level.

Table 3
Sex hormone levels of serum in mice after an intragastric administration with 10 mg/kg BW TiO_2 NPs for the 90 consecutive days.

Sex hormone level	Control	TiO_2 NPs
E_2 (pmol/l)	88.06 ± 4.40	99.01 ± 4.95*
P_4 (nmol/l)	32.10 ± 1.60	27.88 ± 1.39*
LH (IU/l)	0.11 ± 0.005	0.02 ± 0.001**
FSH (IU/l)	0.41 ± 0.021	0.29 ± 0.015*
PRL (μg/l)	0.62 ± 0.031	0.65 ± 0.033
T (ng/dl)	65.26 ± 3.26	54.47 ± 2.72*
SHBG (nmol/l)	0.40 ± 0.02	0.40 ± 0.02

Ranks indicate mean and values represent means ± SE (N = 5).
* Significantly different from experimental groups at the 5% confidence level.
** Significantly different from experimental groups at the 1% confidence level.

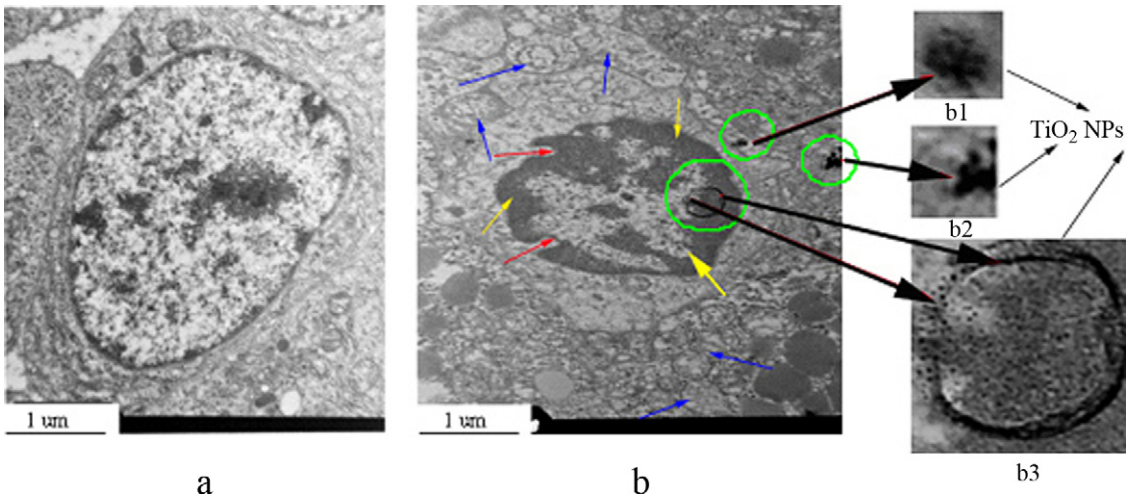

Fig. 2. Ultrastructure of ovarian cell in female mice caused by an intragastric administration with 10 mg/kg BW TiO_2 NPs for 90 consecutive days. (a) Control group: nucleus with homogeneous chromatin, mitochondria turn complete in ovarian cell; (b) TiO_2 NPs group: nuclear membrane collapse (red arrows), chromatin margination (yellow arrows), mitochondria swelling and cristae breakage (blue arrows) in ovarian cell; presence of TiO_2 NPs agglomerates (green cycle). Magnify the green circle indicates that TiO_2 NPs aggregated in the cytoplasm or nucleus of ovarian cell (b1–b3). (For interpretation of the references to color in this figure legend, the reader is referred to the web version of the article.)

4.7. Gene expression profile

The global gene expression profile of ovaries, including the TiO_2 NPs-treated and control groups, was detected using a microarray. Cluster analysis of these ovarian genes revealed significant changes in the levels of expression after TiO_2 NPs exposure, i.e., 223 gene function was up-regulated (diffscore ≥ 13, $P < 0.05$), while 65 genes were down-regulated (diffscore ≤ -13, $P < 0.05$). Furthermore, 10 genes involving hormone levels and reproduction were up-regulated (diffscore ≥ 13, $P < 0.05$; Table 5), and 3 genes were down-regulated (diffscore ≤ -13, $P < 0.05$; Table 5), for example, *Cyp17a1* and *Lgmn* diffscores were 15.75862 and 59.11149, respectively, which were confirmed by RT-PCR assay. 18 genes involving apoptosis were up-regulated (diffscore ≥ 13, $P < 0.05$; Table 5), and 3 genes were down-regulated (diffscore ≤ -13, $P < 0.05$; Table 5), for instance, Bmf diffscore was 19.57678, which was also confirmed by RT-PCR assay. Other differential genes of known function fall in categories involved in response to oxidative stress, immune and inflammatory responses, transcription, ion transport, regulation of cell proliferation, and oxidoreductase activity of ovary (diffscore ≥ 13 or diffscore ≤ -13, $P < 0.05$; Suppl table).

4.8. RT-PCR

To verify the accuracy of the microarray assays, 13 genes that demonstrated significantly different expression patterns were chosen for further RT-PCR assays due to their association with apoptosis, hormone levels, reproduction, response to oxidative stress, regulation of cell proliferation, oxidoreductase activity and transcription. 13 genes were verified by RT-PCR, all of which displayed expression patterns comparable with the microarray data (i.e., either up- or down-regulation; Table 6), with the exception of *Foxn4*, which showed discrepancy between the two methods, suggesting possible problems with RNA handling or pipetting issues.

Table 4
ROS production and DNA peroxidation in ovary of mice after an intragastric administration with 10 mg/kg BW TiO_2 NPs for 90 consecutive days.

Index	Control	TiO_2 NPs
O_2^- (nmol/mg prot min)	18 ± 0.90	87 ± 4.35*
H_2O_2 (nmol/mg prot min)	27 ± 1.35	115 ± 5.75*
8-OHdG (μg/ml)	0.29 ± 0.01	0.84 ± 0.04*

Values represent means ± SE ($N = 10$).
* Significantly different from the control (unexposed mice) at the 1% confidence level.

5. Discussion

In this study, the effects of TiO_2 NPs on ovarian function of female mice were studied. After intragastric administration with 10 mg/kg BW of TiO_2 NPs for 90 consecutive days, titanium was significantly accumulated in the mouse ovaries (Table 1). It was reported that TiO_2 NPs aggregate into units of micrometer size and greater when exposed to calcium and magnesium which would be present in gastric fluids [36,37]; however, aggregation in gastric fluids in mice was not detectable in our laboratory due to current limitations. A future study on how this problem can be circumvented is required. One possible reason is that TiO_2 NPs entered blood circulation from the digestive system and reached the ovaries. In addition, our results also show that exposure to TiO_2 NPs led to increased Ca, Na, K, and Zn contents, and decreased Mg, Cu, and Fe contents (Table 1). The equilibrium of various elements is necessary for immune integrity in organisms. An elemental deficiency or overdosage would impair the physiologic state, decrease immune capacity, and result in disease susceptibility. Moreover, accumulation of TiO_2 NPs caused atresia of primary and secondary follicle development, and induced apoptosis in the ovaries (Figs. 1 and 2).

Recently, Wang et al. [38] demonstrated that chronic exposure to TiO_2 NPs disrupted zebrafish reproduction. Our data also suggest that chronic TiO_2 NPs exposure resulted in a reduction of fertility and development of young mice (Table 2). Follicle development and fertility are associated with the levels of sex hormones. The present study demonstrates that exposure to TiO_2 NPs significantly decreased serum levels of P_4, LH, T, and FSH, and increased the concentration of E_2 (Table 3). In female reproduction, P_4 plays key roles in ovulation, implantation, and maintenance of pregnancy [39], and has been shown to enhance the production of proteolytic enzymes important for the rupture of follicles at ovulation [40]. In the early stages of folliculogenesis, T appears to promote follicular growth and facilitate the response of follicles to FSH. In addition, T has wide ranging roles in ovarian function, including granulosa cells, theca cells, oocytes, and interstitial cells, because T enhances IGF-I and IGF-I receptor mRNAs in primates [41,42]. If

Table 5
Differential expression of known function genes involving hormone levels, reproduction, and apoptosis in ovary of mice after an intragastric administration with 10 mg/kg BW TiO_2 NPs for 90 consecutive days.

Function	Symbol	Name	Diffscore
Steroid metabolic process	Cyp2b10	Cytochrome P450, family 2, subfamily b, polypeptide 10	−15.842
	Lgmn	Legumain	59.11149
	Soat1	Sterol O-acyltransferase 1	17.58913
Estrogen receptor signaling pathway	Safb	Scaffold attachment factor B	15.27988
Parturition	Rxfp1	Relaxin/insulin-like family peptide receptor 1	15.89648
Progesterone metabolic process	Akr1c18	Alde-keto reductase family 1, member C18	142.064
Regulation of hormone levels	Cplx1	Complexin 1	−45.7665
	Adh1	Alcohol dehydrogenase 1	29.58204
	Star	Steroidogenic acute regulatory protein	37.61993
	Cyp11a	Cytochrome P450, family 11, subfamily a	41.38285
	Cyp11a1	Cytochrome P450, family 11, subfamily a, polypeptide 1	15.07402
	Cyp17a1	Cytochrome P450, family 17, subfamily a, polypeptide 1	15.75862
	Safb	Scaffold attachment factor B	15.27988
	Scarb1	Scavenger receptor class B, member 1	29.73179
	Lep	Leptin	−19.0027
Apoptosis	Tsc22d3	TSC22 domain family, member 3	15.75121
	Cfdp1	Craniofacial development protein 1	15.12578
	Comp	Cartilage oligomeric matrix protein	15.71373
	Cryab	Crystalline, alpha B	27.86917
	Pik3ca	Phosphatidylinositol 3-kinase, catalytic, alpha polypeptide	23.02136
	Spp1	Secreted phosphoprotein 1	−27.4615
	Tbx3	T-box 3	15.64415
	Uba52	Ubiquitin A-52 residue ribosomal protein fusion protein fusion product 1	17.47084
	Pik3cg	Phosphoinositide-3-kinase, catalytic, gamma polypeptide	17.17405
	Tchp	Trichoplein, keratin filament binding	20.48037
	Dap	Death-associated protein	17.60245
	Cib1	Calcium and integrin binding 1	16.13592
	Bcl2a1b	B-cell leukemia/lymphoma 2 related protein A1b	17.69281
	Rhob	Ras homolog gene family, member B	18.4887
	Fastkd1	FAST kinase domain 1	32.96398
	Unc5b	unc-5 homolog B	13.08512
	Arhgef16	Rho guanine nucleotide exchange factor (GEF) 16	−13.7839
	Serinc3	Serine incorporator 3	18.26062
	bmf	BCL2 modifying factor	19.57678
	Lcn2	Lipocalin 2	−17.0589
	Id3	Inhibitor of DNA binding 3	20.73859

Values represent means, $N = 3$. We classified the function of these genes according to gene ontology in NCBI (http://www.ncbi.nlm.nih.gov/).

mice lack T and functional androgen receptors, the reproductive lifespan is reduced due to accelerated aging of the ovary and these mice are subfertile [42]. FSH and LH are the major components of the hypothalamic–pituitary–gonadal axis, which regulates reproductive function and ultimately the production of gametes and fertility. E_2 is responsible for facilitating the differentiation of granulosa cells, including the induction of receptor systems for FSH, LH, and PRL, and E_2 can influence post-receptor mechanisms. In conjunction with LH and FSH, E_2 stimulates cAMP accumulation [43] and increases the number of cAMP binding sites in granulosa cells [44]. Therefore, the inhibition of primary and second follicle development and the reduction of fertility caused by TiO_2 NPs exposure were due to alterations of E_2, FSH, P_4, LH, and T levels.

To further confirm ovarian apoptosis, we detected ROS production and DNA damage in the ovary. Oxidative stress is known to induce cellular death by apoptosis or necrosis [45]. Our data showed that significant production of ROS (such as O_2^- and H_2O_2) and DNA peroxidation (8-OHdG increased) occurred in TiO_2 NPs-treated mouse ovaries (Table 4), indicating that these TiO_2 NPs-treated mouse ovaries underwent severe oxidative stress. Nanoparticles have been demonstrated to mediate their toxicity through induction of ROS [46]. Increased cellular ROS levels have been shown to be associated with induction of apoptotic and necrotic cell death in cell cultures [47,48]. Moreover, it has been reported that exposure to TiO_2 NPs resulted in significant production of ROS (OH and O_2^-) in liver, spleen, brain and lung of mice, and caused apoptosis in these organs [13,17,20,49]. ROS generation has also been shown to induce 8-OHdG or 2,6-diamino-4-hydroxy-5-formamidopyrimidine formation [50,51]; however, 8-OHdG is by far the most studied oxidative DNA lesion [52]. In this study, DNA peroxidation in the ovary following exposure to TiO_2 NPs was demonstrated by the enhancement of 8-OHdG (Table 4). This process of ovarian apoptosis caused by TiO_2 NPs may be mediated by the mitochondrial death pathway [17,20].

TiO_2 NPs-induced changes in hormone levels and ovarian injury in mice may be related to alterations in ovarian gene expression. In the current study we therefore investigated all of the genes ($N = 45{,}000$) in the mouse ovary, and the levels of expression of 288 genes of known function were significantly changed by long-term exposure to TiO_2 NPs (Table 5). Table 5 shows the differential expression of genes with known function in categories, and the main results are discussed as follows.

In the current study, *Akr1c18*, *Cyp17a1*, and *Lgmn* were shown to be markedly up-regulated in genes of known function by TiO_2 NPs exposure (Table 5). It is well-known that AKR1C18(20a-HSD), which belongs to the AKR1C protein subfamily, has been identified [53]. Hydroxysteroid dehydrogenase (HSD) belongs to the aldo–keto reductase (AKR) superfamily. Aldo–keto reductases (AKRs) represent a superfamily of monomeric oxidoreductases that catalyze the NADP(H)-dependent reduction of a wide variety of substrates, including simple carbohydrates, steroid hormones, endogenous prostaglandins, and other aliphatic aldehydes and

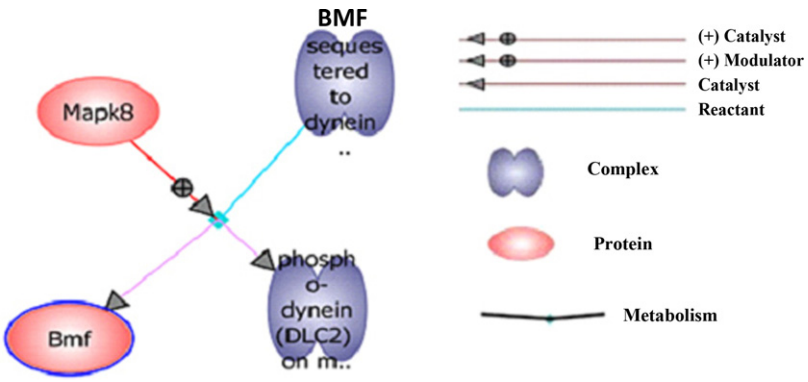

Fig. 3. Pathway of "Activation of BMF and translocation to mitochondria" obtained from network analysis of differentially expressed genes in ovary. MAPK8 phosphorylates BMF sequestered to dynein light-chains 2 (DLC2) on myosin V motor complex, and BMF is unleashed. Gene Spring software was used to construct and visualize molecular interaction networks.

Table 6
Real time quantitative RT-PCR validation of selected genes from microarray data in TiO_2 NPs treated groups.

	ΔΔCt	Fold	Microarray diffscore
Apoe	−0.55534	1.46946704	1.724512
Bmf	−0.44536	1.361655739	2.109554
Calm3	−0.08884	1.06351693	1.674218
Cyp11a	−0.57756	1.49231904	2.911542
Cyp11a1	−0.58492	1.560397941	1.820234
Cyp17a1	−0.71053	1.636404035	1.607409
Cyp2f2	0.756276	0.592022536	0.5654877
Cyp4f18	−4.99464	31.88122148	8.341696
Degs2	0.260948	0.834538204	0.4150108
Foxn4	−0.0654	1.046377918	0.3398899
Lgmn	−1.767	3.4034502	2.555944
Scarb1	−1.32764	2.509914118	33.22819
Star	−1.49024	2.809362906	1.824105

Values represent means ($N = 3$).

ketones [54,55]. AKR1C18 catalyzes the inactivation of progesterone in the ovary, and is distinguished from the enzyme found in other steroidogenic tissues (adrenal and testis) where its principal substrates may be 17α-hydroxypregnenolone or 17α-hydroxyprogesterone. In the ovary, AKR1C18 plays an important role in converting progesterone (a potent progestin) into 20α-hydroxyprogesterone (a weak progestin). Consequently, AKR1C18 plays an important role in the termination of pregnancy and initiation of parturition by reduction of progesterone levels in the serum and placenta. In steroid target tissues, AKR1C18 regulates the amount of progestin that can bind to the progesterone receptor, and in this regard may be important in the placenta and endometrium [56,57]. CYP17A1, also known as cytochrome P450 17A1, steroid 17α-monooxygenase, or 17α-hydroxylase/17, 20 lyase/17, 20 desmolase, is a key enzyme in the steroidogenic pathway that produces progestins, mineralocorticoids, glucocorticoids, androgens, and estrogens. CYP17A1 converts pregnenolone and progesterone to the 17-hydroxy forms, and converts 17-hydroxypregnenolone and 17-hydroxyprogesterone to dehydroepiandrosterone (DHEA) and androstenedione, respectively. *Cyp17a1* encodes a member of the cytochrome P450 superfamily of enzymes. LGMN is also related to the steroid metabolic process and negative regulation of multicellular organism growth, implying that overexpression of *Akr1c18*, *Cyp17a1*, and *Lgmn* results in E_2 elevation and reduction of P_4, LH and T, further leading to inhibition of follicle development (Fig. 1) and decreased fertility of female mice with TiO_2 NPs exposure (Table 2).

In the present study we observed ovarian apoptosis caused by TiO_2 NPs (Fig. 2). To further clarify the molecular mechanism underlying apoptosis, we analyzed the apoptotic genes and showed that 21 genes were altered significantly by TiO_2 NPs exposure (Table 5). It is believed that apoptosis of the ovary initiates atresia in those follicles that serve as the resting pool or are at the earliest stages of maturation [58,59], and apoptosis of the follicular granulosa cells is likely the underlying cause of follicle degeneration [60–63]. Although studies have shown that ovarian cell apoptosis is regulated by an array of extracellular signals through endocrine, autocrine, and paracrine mechanisms in a development-dependent manner [64], insight based on characterization of conserved intracellular effectors has suggested that intracellular pathways leading to apoptosis in diverse organisms are regulated by a group of evolutionarily-conserved genes, including ced3: caspases, ced-4: Apaf-1, and ced-9: Bcl-2 gene families [65–68]. The present data suggest that mRNA levels of the pro-apoptotic BH3-only proteins, Bmf and Bcl2a1b, were up-regulated (Table 5). Activation of BMF and translocation to the mitochondria pathway is presented in Fig. 3. The Bcl2-modifying factor (BMF) is a pro-apoptotic BH3-only member of the Bcl2 family of apoptosis-related proteins, and BMF has been shown to be an apoptotic "trigger" protein that initiates programmed cell death in some epithelial cells [69]. BMF is sequestered to the actin cytoskeleton *in vivo* from a myosin-binding domain (DLC2), and dynein light-chains 2 (DLC2) forms part of the actin-based myosin V motor as well as the microtubular dynein motor complex [69]. When cells are subjected to conditions that induce apoptosis, mitogen-activated protein kinase 8 (MAPK8, also known as JNK1) phosphorylates BMF on specific serine residues located within and directly adjacent to the BMF actin/myosin-binding domain (DLC2) [70,71], and there is loss of actin-BMF sequestration [70]. BMF proceeds to the mitochondria after being freed from actin, and physically interacts with the death-opposing Bcl2 protein, thus triggering the initiation of apoptosis [69]. Thus, apoptosis of mouse ovarian cells caused by exposure to TiO_2 NPs was via activation of BMF and translocation to the mitochondria pathway.

TiO_2 is an inert and poorly soluble matter. A potential exposure route for the general population is oral ingestion as TiO_2 is used as a food additive in toothpaste, capsules, cachou, and so on. The quantity of TiO_2 should not exceed 1% by weight of the food according to the Federal Regulations of the US Government. In 1969, WHO reported that the LD50 of TiO_2 for rats or mice was larger than 12,000 mg/kg BW after oral administration. In the present study, mice were exposed to 10 mg/kg BW TiO_2 NPs every day. This was equal to exposure of approximately 0.6–0.7 g TiO_2 NPs in a human

with a body weight of 60–70 kg, which was a relatively safe dose. However, we think attention should be focused on the application of TiO_2 NPs and their potential long-term exposure effects especially in humans.

In summary, this is the first study to show that TiO_2 NPs can be translocated to ovaries and aggregated within ovarian cells, leading to ovarian dysfunction which may be closely associated with an imbalance of sex hormones and significant alterations in functional gene expression levels in the ovaries of mice.

Acknowledgements

This work was supported by National Natural Science Foundation of China (grant nos. 81273036, 30901218, 30972504, and 81172697), a project funded by the Priority Academic Program Development of Jiangsu Higher Education Institutions, Major State Basic Research Development Program of China (973 Program) (grant no. 2006CB705602), National Important Project on Scientific Research of China (no. 2011CB933404), National New Ideas Foundation of Student of China (grant no. 111028534), and the "Chun-Tsung Scholar" Foundation of Soochow University.

Appendix A. Supplementary data

Supplementary data associated with this article can be found, in the online version, at doi:10.1016/j.jhazmat.2012.08.049.

References

[1] G. Brumfiel, Nanotechnology: a little knowledge, Nature 424 (2003) 246–248.
[2] V.L. Colvin, The potential environmental impact of engineered nanomaterials, Nat. Biotechnol. l21 (2003) 1166–1170.
[3] L.H. Ding, J. Stilwell, T.T. Zhang, O. Elboudwarej, H.J. Jiang, J.P. Selegue, P.A. Cooke, J.W. Gray, F.F. Chen, Molecular characterization of the cytotoxic mechanism of multiwall carbon nanotubes and nano-onions on human skin fibroblast, Nano Lett. 5 (2005) 2448–2464.
[4] T.T. Zhang, J.L. Stilwell, D. Gerion, L.H. Ding, O. Elboudwarej, P.A. Cooke, J.W. Gray, A.P. Alivisatos, F.F. Chen, Cellular effect of high doses of silica-coated quantum dot profiled with high throughput gene expression analysis and high content cellomics measurements, Nano Lett. 6 (2006) 800–808.
[5] J. Jiang, G. Oberdorster, E. Elder, R. Gelein, P. Mercer, P. Biswas, Does nanoparticle activity depend upon size and crystal phase? Neurotoxicology 2 (2008) 33–42.
[6] F. Afaq, P. Abidi, R. Matin, Q. Rahman, Cytotoxicity, pro-oxidant effects and antioxidant depletion in rat lung alveolar macrophages exposed to ultrafine titanium dioxide, J. Appl. Toxicol. 18 (1998) 307–312.
[7] D.B. Warheit, T.R. Webb, K.L. Reeda, S. Frerichs, C.M. Sayes, Pulmonary toxicity study in rats with three forms of ultrafine-TiO_2 particles: differential responses related to surface properties, Toxicology 230 (2007) 90–104.
[8] J.X. Wang, G.Q. Zhou, C.Y. Chen, H.W. Yu, T.C. Wang, Y.M. Ma, G. Jia, Y.X. Gao, B. Li, J. Sun, Y.F. Li, Y.L. Zhao, Z.F. Chai, Acute toxicity and biodistribution of different sized titanium dioxide particles in mice after oral administration, Toxicol. Lett. 168 (2007) 176–185.
[9] D.B. Warheit, R.A. Hoke, C. Finlay, E.M. Donner, K.L. Reed, C.M. Sayes, Development of a base of toxicity tests using ultrafine TiO_2 particles as a component of nanoparticle risk management, Toxicol. Lett. 171 (2007) 99–110.
[10] H.T. Liu, L.L. Ma, J.F. Zhao, J. Liu, J.Y. Yan, J. Ruan, F.S. Hong, Biochemical toxicity of mice caused by nano-anatase TiO_2 particles, Biol. Trace Elem. Res. 129 (2009) 170–180.
[11] L.L. Ma, J.F. Zhao, J. Wang, Y.M. Duan, J. Liu, N. Li, H.T. Liu, J.Y. Yan, J. Ruan, F.S. Hong, The acute liver injury in mice caused by nano-anatase TiO_2, Nanoscale Res. Lett. 4 (2009) 1275–1285.
[12] Y.M. Duan, J. Liu, L.L. Ma, N. Li, H.T. Liu, J. Wang, L. Zheng, C. Liu, X.F. Wang, X.Y. Zhao, J.Y. Yan, S.S. Wang, H. Wang, X.G. Zhang, F.S. Hong, Toxicological characteristics of nanoparticulate anatase titanium dioxide in mice, Biomaterials 31 (2010) 894–899.
[13] N. Li, L.L. Ma, J. Wang, J. Liu, Y.M. Duan, H.T. Liu, X.Y. Zhao, S.S. Wang, H. Wang, F.S. Hong, Y.N. Xie, Interaction between nano-anatase TiO_2 and liver DNA from mice in vivo, Nanoscale Res. Lett. 5 (2010) 108–115.
[14] Y.L. Cui, X.L. Gong, Y.M. Duan, N. Li, R.P. Hu, H.T. Liu, M.M. Hong, M. Zhou, L. Wang, H. Wang, F.S. Hong, Hepatocyte apoptosis and its molecular mechanisms in mice caused by titanium dioxide nanoparticles, J. Hazard. Mater. 183 (2010) 874–880.
[15] H.T. Liu, L.L. Ma, J. Liu, J.F. Zhao, J.Y. Yan, F.S. Hong, Toxicity of nano-anatase TiO_2 to mice: liver injury, oxidative stress, Toxicol. Environ. Chem. 92 (2010) 175–186.
[16] Y.L. Cui, H.T. Liu, M. Zhou, Y.M. Duan, N. Li, X.L. Gong, R.P. Hu, M.M. Hong, F.S. Hong, Signaling pathway of inflammatory responses in the mouse liver caused by TiO_2 nanoparticles, J. Biomed. Mater. Res. A 96 (2011) 221–229.
[17] N. Li, Y.M. Duan, M.M. Hong, L. Zheng, M. Fei, X.Y. Zhao, J. Wang, Y.L. Cui, H.T. Liu, J.W. Cai, S.J. Gong, H. Wang, F.S. Hong, Spleen injury and apoptotic pathway in mice caused by titanium dioxide nanoparticles, Toxicol. Lett. 195 (2010) 161–168.
[18] L.L. Ma, J. Liu, N. Li, J. Wang, Y.M. Duan, J.Y. Yan, H.T. Liu, H. Wang, F.S. Hong, Oxidative stress in the brain of mice caused by translocated nanoparticulate TiO_2 delivered to the abdominal cavity, Biomaterials 31 (2010) 99–105.
[19] R.P. Hu, X.L. Gong, Y.M. Duan, N. Li, Y. Che, Y.L. Cui, M. Zhou, C. Liu, H. Wang, F.S. Hong, Neurotoxicological effects and the impairment of spatial recognition memory in mice caused by exposure to TiO_2 nanoparticles, Biomaterials 31 (2010) 8043–8050.
[20] R.P. Hu, L. Zheng, T. Zhang, Y.L. Cui, G.D. Gao, Z. Cheng, J. Cheng, M.M. Hong, M. Tang, F.S. Hong, Molecular mechanism of hippocampal apoptosis of mice following exposure to titanium dioxide nanoparticles, J. Hazard. Mater. 191 (2011) 32–40.
[21] J.F. Zhao, J. Wang, S.S. Wang, X.Y. Zhao, J.Y. Yan, J. Ruan, F.S. Hong, The mechanism of oxidative damage in nephrotoxicity of mice caused by nano-anatase TiO_2, J. Exp. Nanosci. 5 (2010) 447–462.
[22] S.X. Gui, Z.L. Zhang, L. Zheng, Y.L. Cui, X.R. Liu, N. Li, F.S. Hong, Molecular mechanism of kidney injury of mice caused by exposure to titanium dioxide nanoparticles, J. Hazard. Mater. 195 (2011) 365–370.
[23] R. Stelzer, R.J. Hutz, Gold nanoparticles enter rat ovarian granulosa cells and subcellular organelles, and alter in vitro estrogen accumulation, J. Reprod. Dev. 55 (2009) 685–690.
[24] S.C. Boca, M. Potara, F. Toderas, O. Stephan, P.L. Baldeck, S. Astilean, Uptake and biological effects of chitosan-capped gold nanoparticles on Chinese hamster ovary cells, Mater. Sci. Eng. C 31 (2011) 184–189.
[25] X.H. Liu, X.Q. Ding, Y.G. Cui, L. Chen, H. Li, Z. Chen, L. Gao, Y. Li, J. Liu, The effect of calcium phosphate nanoparticles on hormone production and apoptosis in human granulosa cells, Reprod. Biol. Endocrinol. 8 (2010) 32–39.
[26] J. Jiang, J. Wang, X.M. Zhang, K.F. Huo, H.M. Wong, K.W.K. Yeung, W.J. Zhang, T. Hu, P.K. Chu, Activation of mitogen-activated protein kinases cellular signal transduction pathway in mammalian cells induced by silicon carbide nanowires, Biomaterials 31 (2010) 7856–7862.
[27] H. Suzuki, T. Toyooka, Y. Ibuki, Simple and easy method to evaluate uptake potential of nanoparticles in mammalian cells using a flow cytometric light scatter analysis, Environ. Sci. Technol. 41 (8) (2007) 3018–3024.
[28] A.L. Di Virgilio, M. Reigosa, P.M. Arnal, M. Fernández Lorenzo de Mele, Comparative study of the cytotoxic and genotoxic effects of titanium oxide and aluminium oxide nanoparticles in Chinese hamster ovary (CHO-K1) cells, J. Hazard. Mater. 177 (2010) 711–718.
[29] P. Yang, C. Lu, N. Hua, Y. Du, Titanium dioxide nanoparticles co-doped with Fe^{3+} and Eu^{3+} ions for photocatalysis, Mater. Lett. 57 (2002) 794–801.
[30] National Institutes of Health (NIH), Guide for the Care and Use of Laboratory Animals, National Academy Press, Washington, DC, 1996.
[31] X.Z. Sang, L. Zheng, Q.Q. Sun, N. Li, Y.L. Cui, R.P. Hu, G.D. Gao, Z. Cheng, J. Cheng, S.X. Gui, H.T. Liu, Z.L. Zhang, F.S. Hong, The chronic spleen injury of mice following long-term exposure to titanium dioxide nanoparticles, J. Biomed. Mater. Res. A 100 (4) (2012) 894–902.
[32] J.E. Kacharmina, P.B. Crino, J. Eberwine, Preparation of cDNA from single cells and subcellular regions cDNA Preparation Characterization, vol. 303, 1999, pp. 3–18.
[33] L.D. Ke, Z. Chen, W.K.A. Yung, A reliability test of standard-based quantitative PCR: exogenous vs endogenous standards, Mol. Cell. Probes 14 (2) (2000) 127–135.
[34] W.H. Liu, D.A. Saint, Validation of a quantitative method for real time PCR kinetics, Biochem. Biophys. Res. Commun. 294 (2) (2002) 347–353.
[35] K.J. Livak, T.D. Schmittgen, Analysis of relative gene expression data using real-time quantitative PCR and the 2(T)(−Delta Delta C) method, Methods 25 (4) (2001) 402–408.
[36] C. Buzea, I.I. Pacheco Blandino, K. Robbie, Nanomaterials and nanoparticles: sources and toxicity, Biointerphases 2 (4) (2007) 1–103.
[37] Y. Hedberg, J. Hedberg, I.O. Wallinder, Particle characteristics and metal release from natural rutile (TiO_2) and zircon particles in synthetic body fluids, J. Biomater. Nanobiotechnol. 3 (2012) 37–49.
[38] J.X. Wang, X.S. Zhu, X.Z. Zhang, Z. Zhao, H.A. Liu, Disruption of zebrafish (*Danio rerio*) reproduction upon chronic exposure to TiO_2 nanoparticles, Chemosphere 83 (2011) 461–467.
[39] J.D. Graham, C.L. Clarke, Physiological action of progesterone in target tissues, Endocr. Rev. 18 (1997) 502–519.
[40] J. Iwamasa, S. Shibata, N. Tanaka, K. Matsuura, H. Okamura, The relationship between ovarian progesterone and proteolytic enzyme activity during ovulation in the gonadotrophin-treated immature rat, Biol. Reprod. 46 (1992) 309–313.
[41] K.A. Vendola, J. Zhou, J. Wang, C.A. Bondy, Androgens promote insulin-like growth factor-I, insulin-like growth factor-I receptor gene expression in the primate ovary, Hum. Reprod. 14 (1999) 2328–2332.
[42] K.A. Vendola, J. Zhou, J. Wang, O.A. Famuyiwa, M. Bievre, C.A. Bondy, Androgens promote oocyte insulin-like growth factor 1 expression and initiation of follicle development in the primate ovary, Biol. Reprod. 61 (1999) 353–357.
[43] M.F. Lyon, P.H. Glenister, Reduced reproductive performance in androgen-resistant Tfm/Tfm female mice, Proc. R. Soc. Lond. B: Biol. Sci. 208 (1980) 1–12.

[44] J.S. Richards, J.A. Jonassen, A.I. Rolfes, K. Kersey, L.E. Reichert Jr., Adenosine 3′,5′-monophosphate, LH receptor and progesterone during granulosa cell differentiation: effects of oestradiol and FSH, Endocrinology 104 (1979) 765–770.
[45] J.S. Richards, A.I. Rolfes, Hormonal regulation of cyclic AMP binding to specific receptor proteins in rat ovarian follicles, J. Biol. Chem. 225 (1980) 5481–5489.
[46] D.M. Hockenbery, Z.N. Oltvai, X.M. Yin, C.L. Milliman, S.J. Korsmeyer, Bcl-2 functions in an antioxidant pathway to prevent apoptosis, Cell 75 (1993) 241–251.
[47] A. Nel, T. Xia, L. Madler, N. Li, Toxic potential of materials at the nanolevel, Science 311 (5761) (2006) 622–627.
[48] S. Ueda, H. Masutani, H. Nakamura, T. Tanaka, M. Ueno, J. Yodoi, Redox control of cell death, Antioxid. Redox Signal. 4 (3) (2002) 405–414.
[49] M. Ott, V. Gogvadze, S. Orrenius, B. Zhivotovsky, Mitochondria, oxidative stress and cell death, Apoptosis 12 (5) (2007) 913–922.
[50] Q.Q. Sun, D.L. Tan, Q.P. Zhou, X.R. Liu, Z. Cheng, G. Liu, M. Zhu, X.Z. Sang, S.X. Gui, J. Cheng, R.P. Hu, M. Tang, F.S. Hong, Oxidative damage of lung and its protective mechanism in mice caused by long-term exposure to titanium dioxide nanoparticles, J. Biomed. Mater. Res. A 100 (10) (2012) 2554–2562.
[51] A.P. Grollman, M. Moriya, Mutagenesis by 8-oxoguanine: an enemy within, Trends Genet. 9 (1993) 246–249.
[52] M.D. Evans, M. Dizdaroglu, M.S. Cooke, Oxidative DNA damage and disease: induction, repair and significance, Mutat. Res. 567 (2004) 1–6.
[53] A. Pilger, W.H. Rüdiger, 8-Hydroxy-2′-deoxyguanosine as a marker of oxidative DNA damage related to occupational and environmental exposures, Int. Arch. Occup. Environ. Health 80 (2006) 1–15.
[54] M. Ishida, K.T. Chang, I. Hirabayashi, M. Nishihara, M. Tkahashi, Cloning of mouse 20a-hydroxysteroid dehydrogenase cDNA and its mRNA localization during pregnancy, J. Reprod. Dev. 45 (1999) 321–329.
[55] Z. Krozowski, The short-chain alcohol dehydrogenase superfamily: variations on a common theme, J. Steroid Biochem. Mol. Biol. 51 (1994) 125–130.
[56] H. Jornvall, B. Persson, M. Krook, S. Atrian, R. Gonzalez-Duarte, J. Jeffery, D. Ghosh, Short-chain dehydrogenases/reductases (SDR), Biochemistry 34 (1995) 6003–6013.
[57] T.M. Penning, Molecular endocrinology of hydroxysteroid dehydrogenases, Endocr. Rev. 18 (1997) 281–305.
[58] J. Mao, R.W. Duan, L. Zhong, G. Gibori, S. Azhar, Expression, purification and characterization of the rat luteal 20 alpha-hydroxysteroid dehydrogenase, Endocrinology 138 (1997) 182–190.
[59] G.I. Perez, R. Robles, C.M. Knudson, J.A. Flaws, S.J. Korsmeyer, J.L. Tilly, Prolongation of ovarian lifespan into advanced chronological age by Bax-deficiency, Nat. Genet. 21 (1999) 200–203.
[60] A. Gougeon, Regulation of ovarian follicular development in primates: facts and hypotheses, Endocr. Rev. 17 (1996) 121–155.
[61] A.L. Johnson, Intracellular mechanisms regulating cell survival in ovarian follicles, Anim. Reprod. Sci. 78 (2003) 185–201.
[62] J.L. Tilly, K.I. Kowalski, A.L. Johnson, A.J.W. Hsueh, Involvement of apoptosis in ovarian follicular atresia and postovulatory regression, Endocrinology 129 (1991) 2799–2801.
[63] HughesF F.M. Jr., W.C. Gorospe, Biochemical identification of apoptosis (programmed cell death) in granulosa cells: evidence for a potential mechanism underlying follicular atresia, Endocrinology 129 (1991) 2415–2422.
[64] A.J.W. Hsueh, K. Eisenhauer, S.Y. Chun, S.Y. Hsu, H. Billig, Gonadal cell apoptosis, Recent Prog. Horm. Res. 51 (1996) 433–455.
[65] M.S. Spector, S. Desnoyers, D.J. Hoeppner, M.O. Hengartner, Interaction between the *C. elegans* cell-death regulators CED-9 and CED-4, Nature 385 (1997) 653–656.
[66] J. Yuan, H.R. Horvitz, The *Caenorhabditis elegans* cell death gene ced-4 encodes a novel protein and is expressed during the period of extensive programmed cell death, Development 116 (1992) 309–320.
[67] J. Yuan, S. Shaham, S. Ledoux, H.M. Ellis, H.R. Horvitz, The *C. elegans* cell death gene ced-3 encodes a protein similar to mammalian interleukin-1-converting enzyme, Cell 75 (1993) 641–652.
[68] M.O. Hengartner, H.R.C. Horvitz, Elegans cell survival gene ced-9 encodes a functional homolog of the mammalian protooncogene bcl-2, Cell 76 (1994) 665–676.
[69] H. Puthalakath, A. Villunger, L.A. O'Reilly, J.G. Beaumont, L. Coultas, R.E. Cheney, D.C. Huang, A. Strasser, BMF: a proapoptotic BH3-only protein regulated by interaction with the myosin V actin motor complex, activated by anoikis, Science 293 (2001) 1829–1832.
[70] H. Kanda, M. Miura, Regulatory roles of JNK in programmed cell death, J. Biochem. 136 (2004) 1–6.
[71] K. Lei, R.J. Davis, JNK phosphorylation of Bim-related members of the BCL2 family induces Bax-dependent apoptosis, Proc. Natl. Acad. Sci. U.S.A. 100 (2003) 2432–2437.